Physical and chemical analysis of a Ni–H_2 cell*

H. Vaidyanathan**, **M. W. Earl** and **T. D. Kirkendall**
COMSAT Laboratories, 22300 Comsat Drive, Clarksburg, MD 20871-9475 (U.S.A.)

Abstract

A cycled aerospace nickel–hydrogen (Ni–H_2) cell was subjected to destructive physical analysis to determine the reason for a capacity loss after 5967 cycles at 60% depth of discharge. The positive plates in the cell were analyzed in terms of chemical composition, active material utilization, charge efficiency and thickness increase. The microstructure of a cross section of the positive plate was determined by backscattered electron image analysis. The results suggest that the capacity loss in the cell is caused by low charge acceptance and low active material utilization at the positive plate. The oxidized nickel species content of the positive plate increased due to corrosion of the nickel sintered skeleton. This appears to circumvent the orderly reaction of the active material. Microstructural analysis has indicated that a new phase of active material is formed with cycling.

Introduction

Tear-down analysis of an aerospace rechargeable cell is normally carried out for purposes such as preflight evaluation of design and manufacturing techniques, tracking the degradation of components in a life test experiment, and determining the reason for failure. The major elements of such an analysis include physical measurements at the cell level, as well as chemical, microstructural and specialized examination of cell components. Some of the procedures used to analyze the cell are an extension of those used for aerospace nickel–cadmium (Ni–Cd) cells and are documented in the literature [1, 2].

Since nickel–hydrogen (Ni–H_2) cells last longer and cycle longer than any other battery, there is tremendous interest in understanding their gradual degradation with cycling and their failure mechanisms. Premature failure of Ni–H_2 cells in a cycling experiment has been reported, and in one instance the failure was attributed to the rapid reaction of oxygen with hydrogen [3]. In the study described here, a flight-model Ni–H_2 cell, which was cycled in a simulated low earth orbit (LEO) regime at 4% overcharge and 60% depth of discharge (DOD) for 5967 cycles, was analyzed to determine the reason for capacity decline.

*This paper is based on work performed at COMSAT Laboratories under the sponsorship of the World Systems Division of the Communications Satellite Corporation.

**Author to whom correspondence should be addressed.

0378-7753/91/$3.50

Electrochemical performance

The subject cell is a COMSAT/INTELSAT design which has asbestos separators in a back-to-back stack configuration. The cell was withdrawn from a LEO cycling test when its end-of-discharge voltage decreased below 1.0 V. Details and pertinent observations made during the LEO test are given in ref. 4. As a first step, cell capacity was determined using a charge rate of $C/10$ and a discharge rate of $C/2$ at 10 °C. Figure 1 compares the voltage profile of the cell at the beginning of the cycling and after 5967 cycles. As a result of cycling, the cell exhibited markedly lower discharge capacity, lower discharge voltages, and higher charge voltages. It is apparent from the capacity decay curve presented in Fig. 2 that cell capacity declined gradually after about 3000 cycles. The cell was subjected to open-circuit stand in the fully charged condition at 10 °C. More than 79% of the cell capacity was retained after 72 h of stand, which is comparable to the value

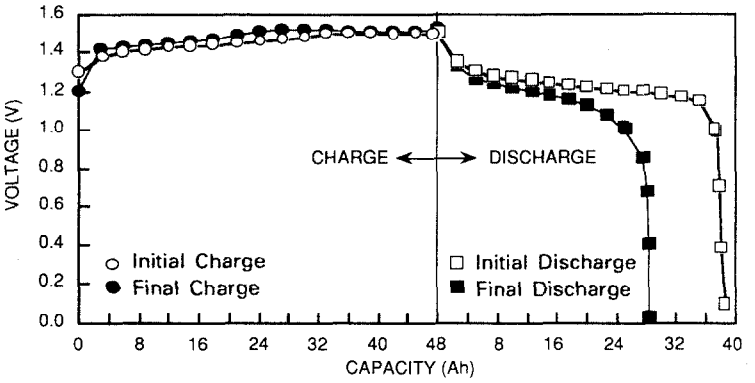

Fig. 1. Charge /discharge voltage profiles for the cell before and after cycling.

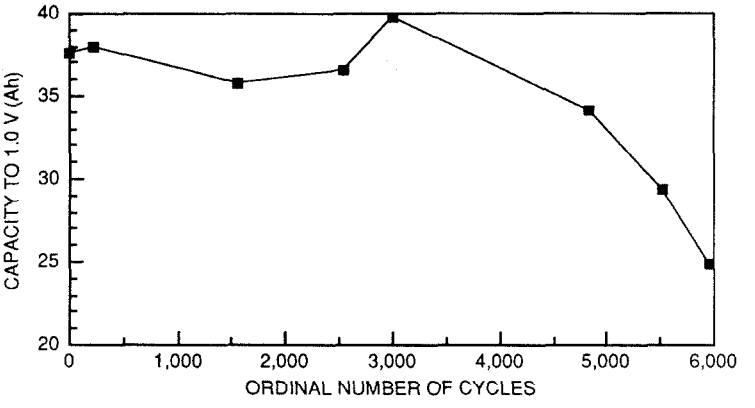

Fig. 2. Variation of capacity (1.0 V) with cycling (discharge rate $C/2$).

exhibited at the beginning of cycling. Thus, the capacity decay in the cell cannot be attributed to soft shorts.

Cell dissection

The cell was dissected and the stack was transferred to a Soxhlet extractor. After extraction of the electrolyte, the stack was dried and disassembled. Examination of cell mechanical components such as the seals, end plates, center rod, inside can wall, weld ring and bus bars did not reveal any damage due to cycling. Evaluation of the anodes, cathodes and separator from the cell revealed the following:

- sticking of the separator to the positive and negative plates; however, no fluidization of asbestos or diffusion of asbestos particles through either electrode was observed
- melted areas comprising 30% of the polypropylene gas distribution screen
- burn holes in the negative plates, and several cracks and delamination in the Gore-Tex™ backing
- a high degree of extrusion of active material in the positive plates

The sticking of the separator probably occurred as a result of compression in the stack. The burn holes and melted areas indicate abnormal heat generation. Delamination of the Gore-Tex™ probably occurred as a result of a rapid oxygen and hydrogen reaction.

Analysis of positive plates

The positive plates were based on slurry plaque impregnated with $Ni(OH)_2$ and $Co(OH)_2$ using an aqueous electrochemical technique. They were analyzed to determine changes in their physical, chemical and microstructural properties, as described below.

Swelling

The thickness of the plates was measured and compared against values obtained for similar uncycled plates. Swelling was calculated to be 10.5%. One important effect of swelling is compression in the stack, which leads to squeezing of the separator, thereby reducing the amount of electrolyte at the interface.

Electrolyte absorbency

The amount of 30% KOH absorbed by a plate was determined using an immersion technique. A value of 0.20 g of KOH per gram of plate was obtained, which was 23% higher than the absorbency of an uncycled plate. It was concluded that swelling of the positive plate leads to an increased number of voids in the positive plates, which capture electrolyte from the separator. In others words, the electrolyte in the stack components is redistributed in the cell.

Chemical composition and active material

The positive plate was quantitatively analyzed, first by extracting the active material with acetic acid, and later by dissolving in HNO_3. The percentage of nickel and cobalt was then determined using atomic absorption spectroscopy. The amount of oxidized nickel species such as active $Ni(OH)_2$ was 22% higher in the cycled plate than in an uncycled positive plate, while the metallic nickel content due to the plaque structure had decreased by approximately a stoichiometrically equivalent amount. This was direct evidence of corrosion of the sintered plaque skeleton.

The porous sintered plaque void volume was calculated based on analytical data and thickness, yielding a value of 25% higher than the void volume of the sintered plaque that was used prior to electrochemical impregnation. This value is in agreement with the increased plate electrolyte absorption discussed earlier. The loading of the active material ($Co(OH)_2$ and $Ni(OH)_2$) was 1.57 g/cm^3 of void – a value close to that for the uncycled plate. Therefore, the increase in void volume due to corrosion and swelling was offset by the increased amount of oxidized nickel species resident in the pores.

Electrochemical properties

The capacity of the plate in 30% KOH was determined at 10 °C to be 1.30 A h, which is 15% less than the minimum capacity obtained for plates of similar design. When this value is factored into Faraday's law, a value of 81.6% is obtained for oxidized nickel species utilization, which is lower than the 115% obtained for an uncycled plate. The reported utilization in excess of 100% is due to the difference between the assumed valency change of 1 and the actual valency change, which is between 1 and 2. Even though the mass of the oxidized nickel species has increased by 22%, it is clear that this material is not available electrochemically. On the contrary, it appears that the presence of this corrosion product and the loss of conductive metallic nickel hinders the charge transfer reaction of the original active material. The charge efficiency of the plate was determined by charging at $C/10$ to a 50% state of charge, and capacity was determined by discharging at $C/2$. The charge efficiency was 81%, as compared to 100% for an uncycled plate.

Microstructural analysis

An image analysis technique based on computer analysis of digitized backscattered electron (BSE) images generated in a scanning electron microscope was employed to study the cross section of the positive plate [5]. Samples were prepared for analysis by encapsulating positive plate sections in epoxy and then cross-sectioning them using metallographic polishing

techniques. In the BSE micrograph of a positive plate cross section (Fig. 3), the gray level is directly related to the local composition of the plate. White areas indicate nickel sinter, gray areas indicate active material, and black areas indicate voids (which were filled with epoxy in the sample preparation step). The most remarkable features of this micrograph are the segregation of active material near the surface, the presence of voids, an increase in thickness, and a blistered region close to the surface.

The active material component can be separated from the sinter and voids and displayed separately by computer selection of the gray level in the digitized BSE image. Figure 4 is a histogram of the gray levels of the 65 536 pixels displayed in the BSE image of Fig. 3. The three peaks correspond

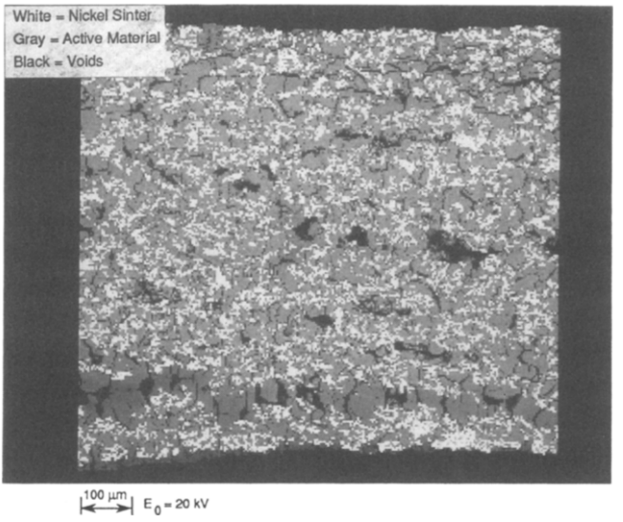

Fig. 3. Digitized BSE image of a cross-sectioned positive plate.

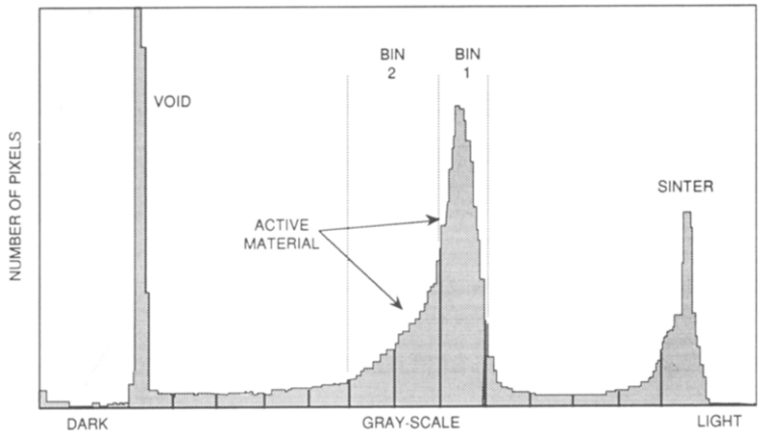

Fig. 4. Histogram of gray levels in the BSE image of the cross-sectioned positive plate shown in Fig. 3.

to voids, active material and sinter particles. By dividing the broad central peak obtained for the active material into separate bins of varying gray level, digitized images of the active material distribution can be obtained. When this selectivity was applied, it was discovered that the active material comprises a range of gray levels in the BSE signal.

Figures 5 and 6 were reconstructed from the BSE image of Fig. 3, using the above selection technique. The distribution of the lighter-appearing active material associated with bin 1 of Fig. 4 is shown in Fig. 5, and the darker active material corresponding to bin 2 is shown in Fig. 6. The lighter active

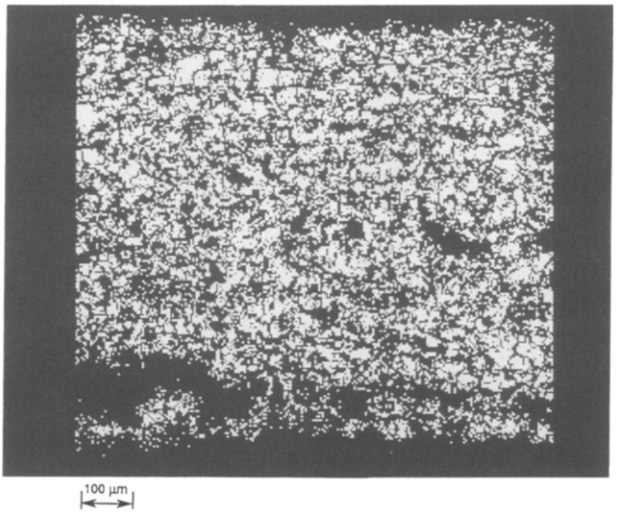

Fig. 5. Active material distribution from bin 1 of Fig. 4.

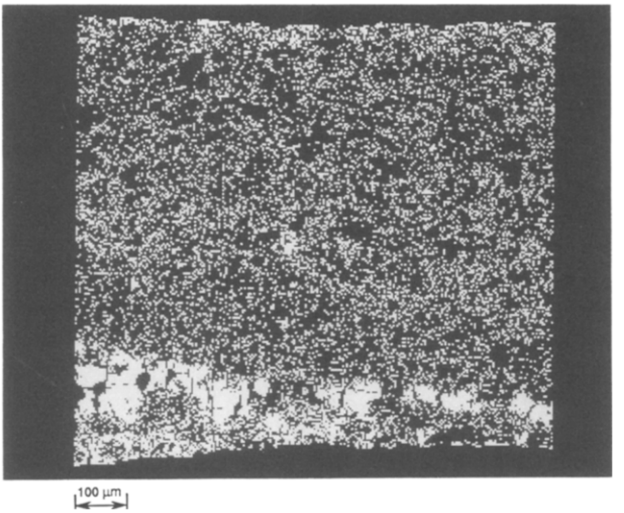

Fig. 6. Lower atomic number active material from bin 2 of Fig. 4.

material is fairly evenly distributed across the plate, except for the blistered region near the edge. This region contains primarily dark active material. Because the scale in the BSE image is a nearly monotonic function of the average atomic number of the local material composition, this variation in the gray level of the active material is interpreted to mean that the blistered region contains active material of a different structure. The difference between this structure and the generally observed active material may be due to the H_2O and KOH content of $Ni(OH)_2$. This chemical change and redistribution of active material has not been observed in uncycled or low-cycled plates.

Cyclic voltammetry

The voltage profile of a miniature (1 cm^2) positive plate was obtained using cyclic voltammetry. The voltage of the test electrode was scanned from -0.5 to $+0.7$ V (versus a Hg/HgO reference electrode) at a rate of 0.1 mV/s in 30% KOH. Figure 7 shows two voltage profiles. Curve A corresponds to an uncycled positive plate, and curve B to a plate from the cycled cell. The uncycled plates exhibited the following features: an anodic peak at $+0.557$ V corresponding to $Ni(OH)_2$ oxidation, another anodic peak at $+0.70$ V corresponding to oxygen evolution, and a cathodic peak at $+0.183$ V corresponding to the reduction of the oxidized active material. The voltage profile of the cycled plate also contains a second cathodic peak which is very broad at -0.120 V. The peaks associated with active material oxidation and reduction are polarized by 19 and 36 mV (respectively) for

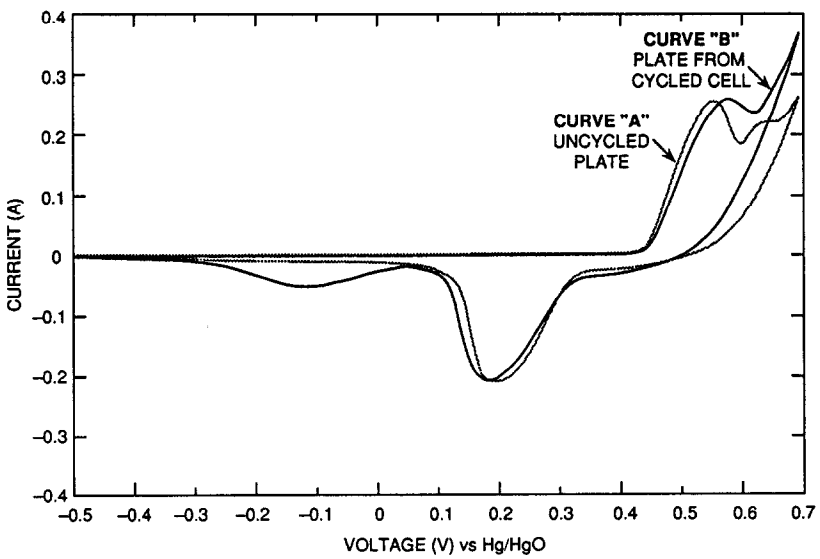

Fig. 7. Voltage profiles of cycled and uncycled positive plates (generated using cyclic voltammetry).

TABLE 1

Changes in positive plate from the cycled cell

Item	Uncycled plate	Cycled plate
Swelling	initial thickness (stable)	10.5% increase in thickness
Electrolyte absorbency (g KOH/g)	0.162	0.20
Plaque porosity (%)	78	80.7
Charge efficiency (%)	100	81
Active material utilization (%)	115	81.6
BSE image analysis	gray active material	gray and dark active material
Cyclic voltammetry	no second cathodic peak	second cathodic peak at −0.120 V

the cycled plate, compared to the uncycled plate. The second cathodic peak could be due to the reduction of a new phase of charged active material which reacts at a much lower cathodic potential. This may be the phase of active material identified in the BSE image analysis.

The results of the positive plate analysis are summarized in Table 1.

Analysis of electrolyte

The electrolyte obtained from the Soxhlet extraction was analyzed for KOH and carbonate. The alkali content (OH, HCO_3, and CO_3^{2-} was 41.31%, of which 3% was carbonate. The electrolyte content translates into 2.92 cm^3/A h. There were no abnormalities in the carbonate content or in the normalized volume per ampere-hour of theoretical capacity.

Discussion

The objective of this study was to explain the decline in capacity and average discharge voltage of a Ni–H_2 cell after 5967 cycles. In addition to close examination of the electrode stack, a range of experiments were conducted to probe the positive plate. The results show that the sintered plaque has corroded, producing additional oxidized nickel species which do not contribute to usable capacity. Also, the plate has swelled, the active material is extruding and electrolyte absorbency has increased. Digitized BSE analysis was used to obtain chemical information, based on the fact that the yield in number of electrons backscattered from a material increases with the average atomic number. BSE image analysis shows two types of active material. This observation, in combination with the second cathodic peak obtained in the cyclic voltametry, suggests that a new phase of active

material is produced with cycling which contains more water, hydroxyl or potassium. The lower charge efficiency and lower active utilization can be attributed to a combination of factors, including the formation of a new phase, as well as slightly lower electrolyte content in the separator as a result of squeezing. The lower charge efficiency has resulted in the production of more oxygen, which is given off in streams and reacts with hydrogen, producing pops (microexplosions) that damage the negative electrode backing layer.

Conclusions

A systematic and regular analysis of a Ni–H_2 cell which exhibited gradual degradation in performance for 5967 cycles has shown that the origin of the failure resides in the positive plates. The conspicuous signs of degradation, such as lower charge efficiency and lower active material utilization of the positive plate, are explained by hypothesizing the formation of a new structure which contains more hydroxyl and potassium. The oxidized nickel species have increased in the positive plate and appear not only to be less active electrochemically, but also to impede the activity of otherwise good $Ni(OH)_2$.

Acknowledgements

The authors wish to thank the following colleagues for their contributions: B. Shaw for BSE analysis, K. Burch for chemical analysis and W. Nakhleh for cyclic voltametric experiments.

References

1 J. D. Dunlop and M. Earl, Evaluation of INTELSAT IV Ni/Cd cells, *Proc. 25th Power Sources Symp.*, PSC Publication Committee, Red Bank, NJ, 1972, pp. 40–42.
2 G. Halpert and V. Kunnigahalli, Procedures for analysis of Ni/Cd cell materials, *NASA Publication X-711-74-279*, NASA-Goddard Space Flight Center, Greenbelt, MD, 1980.
3 K. H. Fuhr, Failure analysis of 3.5 inch, 50 A h nickel–hydrogen cells undergoing low earth orbit testing, *Proc. 22nd Intersociety Energy Conversion Engineering Conf.*, Philadelphia, PA, Aug. 1987, AIAA, New York, pp. 889–892.
4 H. Vaidyanathan, Effect of design variables on the cycling characteristics of Ni/H_2 cells, *Proc. 24th Intersociety Energy Conversion Engineering Conf., Washington, DC, Aug. 1989*, IEEE, New York, pp. 1405–1409.
5 T. P. Remmel and T. D. Kirkendall, in A. D. Romig and J. I. Goldstein (eds.), *Microbeam Analysis*, San Fransisco Press, 1984, pp. 165–168.